Acta Chemica Scandinavica A 39 (1985) 397–403

The Relation between Structure and Composition of Intergrowth Tungsten Bronzoids

RENU SHARMA

Department of Inorganic Chemistry, Arrhenius laboratory, University of Stockholm, S-106 91 Stockholm, Sweden

Different intergrowth tungsten bronzoids ($Cs_xNb_xW_{1-x}O_3$, x=0.08–0.12) can be distinguished only by high resolution electron microscopy (HREM). Energy dispersive X-ray analysis has been used to study the local composition of individual crystal from different phases in the same sample, identified by HREM. The tunnels in the HTB-type slabs are occupied by alkali only to approximately 60 % in all ITB bronzoids studied, just as in the corresponding HTB-type bronzoids. A particular ITB structure probably develops to give the most favourable occupancy with the amount of alkali available.

Tungsten bronzes are non-stoichiometric compounds with the general formula A_xWO_3, where A is typically an alkali metal. Among the different structure types is the hexagonal tungsten bronze, HTB, which forms with the heavy alkali metals K, Rb or Cs for compositions in the range $0.19<x<0.33$.[1] Another type, intergrowth tungsten bronze, ITB, has recently been prepared in the low-alkali region ($x\sim0.1$) with the same heavy alkali elements.[2] These compounds are reduced, with the degree of reduction depending upon the amount of alkali present. They have been reviewed recently by Kihlborg.[3]

Fully oxidised phases can be prepared by replacing part of the hexavalent tungsten by a pentavalent metal to match the alkali content. They have the general formula $A_xT_xW_{1-x}O_3$, and have been prepared for T=V, Ta or Nb. These compounds are isostructural with the true bronzes and can be called 'bronzoids'.[4] HTB bronzoids have been known for some time. They are reported to form with the heavy alkali metals for compositions in the range $0.20<x<0.33$ at 900 °C.[5,6] ITB bronzoids have also recently been observed.[7] Fig. 1a and 1b show the structure model and the corresponding electron micrograph, respectively, of an ITB bronzoid. Like the corresponding true bronze, it can be described in terms of slabs of WO_3 and HTB structure elements, interleaved as seen in Fig. 1a.

Intergrowth bronzes show a variation in the width of the WO_3- and HTB-type slabs, which gives rise to a family of closely related structures. The bronzoids exhibit a much wider range than the true bronzes. In ordered crystal fragments the width of the HTB slabs may vary from 2 to 5 tunnel rows and of the WO_3-type slabs from 2 to 9 octahedra. Disordered crystal fragments have been observed, ranging from those with only a few tunnel rows present here and there in an otherwise perfect WO_3 matrix to HTB with only occasional slices of extra octahedra inserted between the tunnels.[7] Different members of the family can be described by a general notation of the sequence as $(m,n,p\ldots)$,[2] which designates the number of octahedral sheets between the centres of the tunnels. The member shown in the

0302-4377/85 $2.50

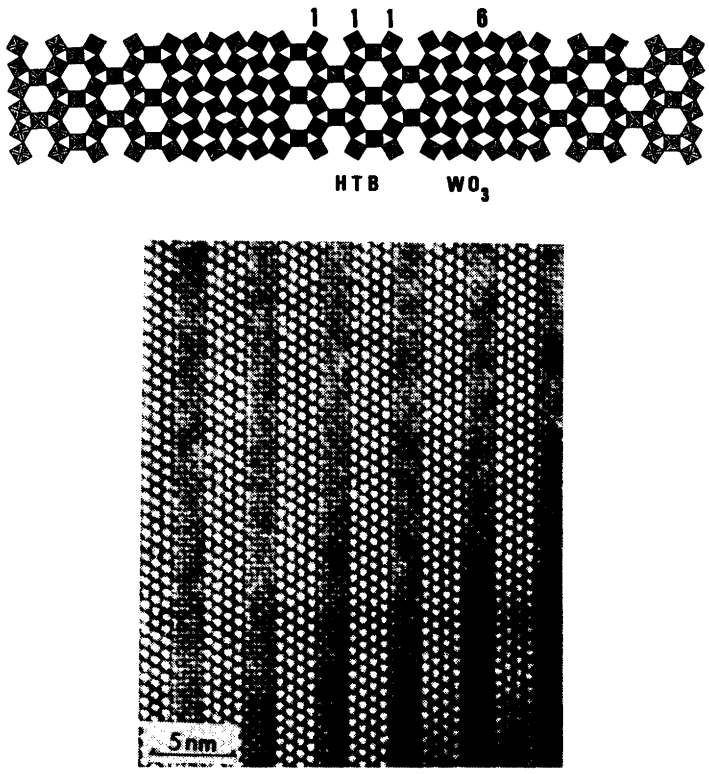

Fig. 1. (a) The structure model, (b) The electron micrograph, of (1,1,1,6)-type ITB (see text).

Fig. 1 should thus be designated as (1,1,1,6). Generally, phases such as this one with quadruple-tunnel rows are written (1,1,1,*n*); with triple-tunnels, (1,1*n*) *etc.*

The alkali metal atoms occupy the tunnel sites of the HTB parts. It is thus probable that the amount of alkali in these phases is correlated with the number of tunnels in the structure. In the pure tungsten bronze of the HTB type, prepared at high temperature, there is a homogeneity range from $x=0.19$ to $x=0.33$, which implies a varying degree of filling of the tunnel sites.[8] With the maximum alkali content, $x=\frac{1}{3}$, all the tunnels are completely filled. In the alkali-niobium-tungsten bronzoid system at 1200 °C, the HTB phase has a very narrow range of homogeneity around $x=0.20$, which indicates a partial occupancy of 60 % of the tunnel sites. For the ITB phases the study of a possible correlation between the alkali content and the structure is complicated by the fact that it has not been possible to prepare the various members as single-phase samples. They always form as a mixture, and the analysis thus has to be performed on individual crystals whose structure can be identified. Micro-analysis by means of energy-dispersive X-ray spectroscopy combined with high resolution electron microscopy (HREM) and electron diffraction has therefore been made on ITB-type crystals. The results are presented below.

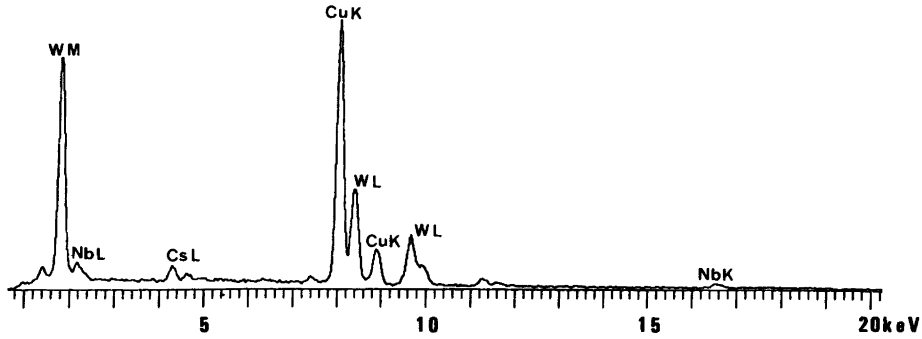

Fig. 2. A characteristic X-ray spectrum from an ordered (1,1,6)-type ITB crystal fragment.

EXPERIMENTAL

Appropriate amounts of Cs_2WO_4, WO_3 and Nb_2O_5 were mixed thoroughly and heated in closed platinum ampoules for 24 h at 1200 °C. A closed system for the preparation was preferred in order to prevent the evaporation and/or reduction of tungsten trioxide. The overall composition of the samples aiming at ITB bronzoids corresponded to $x=0.08-0.12$, which is the range where these phases are most abundant.[7] Samples were also made with $x=0.20$ in order to produce single-phase HTB-type bronzoids. One of the samples (with $x=0.10$) was remixed after annealing and reheated several times for a total of 10 days.

The samples for the HREM study were prepared by crushing the products in an agate mortar, and dispersing a drop of the suspension in n-butanol on a copper-supported holey carbon grid. A Siemens ELMISKOP 102, equipped with a double tilt-lift stage (operated at 125 kV) was utilized as the main tool for high resolution imaging and electron diffraction studies. Thin crystal flakes were selected and identified by their electron diffraction patterns and high resolution images using the technique described in detail by Iijima.[9]

The energy-dispersive X-ray spectra of ordered crystal fragments of known structure, identified by electron diffraction patterns (EDP) and high resolution electron microscopy (HREM), were collected on a PHILIPS EM301 microscope, operated at 80 kV. The equipment included a beryllium holder, a top-hat condenser aperture, an analysis system (EDX LINK-860 Series 2) and a lithium drifted silicon detector (resolution 148 eV for the MnK line). The specimen grid was tilted at an angle of 42° in order for the detector to receive the maximum intensity of characteristic X-rays emitted. The thin-crystal approximation should be valid, as all the crystal flakes used for analysis were the ones suitable for HREM (50–100 Å thick). Quantitative analysis could therefore be done by the ratio method, applicable to thin crystals, for which absorption and fluorescence effects are not severe. In the thin-crystal limit, the concentration ratio of two elements present, x and y, is directly proportional to the intensity ratio of their characteristic X-ray emission lines:

$$C_x/C_y=K_{xy}(I_x/I_y)$$

where $K_{xy}=k_x/k_y$. The constants k_x and k_y are dependent on the intensities generated and the efficiency of the detector to measure them.[10,11] The value of K_{xy} is constant under the same experimental conditions i.e. accelerating voltage, depth of Si dead layer, thickness of Be window etc. It was theoretically calculated by comparing the relative efficiency of the detector for SiK line and for a particular element and spectral line to be used for analysis,[12] since no suitable stoichiometric compounds were available to be used as standards. CsL, NbL and WM lines were measured and used for the calculations. The reliability of the the Nb analysis is rather poor as compared to Cs, due to partial overlap between the WM and NbL peaks. The NbK peak (16.6 eV) could not be used, since it lies in the low-reliability region, with a low peak/background ratio. A typical spectrum is shown in Fig. 2. The CuK lines come from the grid.

Table 1. Observed and calculated Cs content for different phases.

Structure type	No. of HTB rows (M)	No. of octahedra rows (n)	No. of crystals observed	Mean Cs content obs. $(\bar{x})^a$	Standard deviation s^b	Calculated Cs content for 65 % occ.	Calculated Cs content for full occ.	Observed Nb content s^a	Standard deviation s^b
HTB single phase sample		1	6	0.218(10)	0.015	0.216	0.333	0.18(3)	0.032
HTB multi phase sample		1	2	0.168(10)	0.009	0.216	0.333	0.16(3)	0.023
1,1,1,6	4	6	7	0.101(8)	0.008	0.118	0.1818	0.10(3)	0.009
1,1,6	3	6	6	0.097(10)	0.010	0.102	0.158	0.09(3)	0.002
1,1,5	3	5	4	0.106(9)	0.008	0.114	0.176	0.07(3)	0.002
1,1,4	3	4	3	0.129(11)	0.015	0.130	0.200	0.09(3)	0.002
1,1,3	3	3	3	0.118(10)	0.006	0.145	0.230	0.09(3)	0.014
1,7	2	7	2	0.078(11)	0.010	0.072	0.111	0.04(4)	0.022
1,5	2	5	3	0.080(10)	0.007	0.093	0.143	0.05(3)	0.016
1,4	2	4	1	0.095(9)	–	0.108	0.167	0.07(3)	
1,3	2	3	2	0.106(9)	0.007	0.130	0.200	0.09(3)	0.009

[a] Mean deviations within parentheses. [b] Variance $s = \frac{1}{n-1}\sum_i (x_i - \bar{x})^2$.

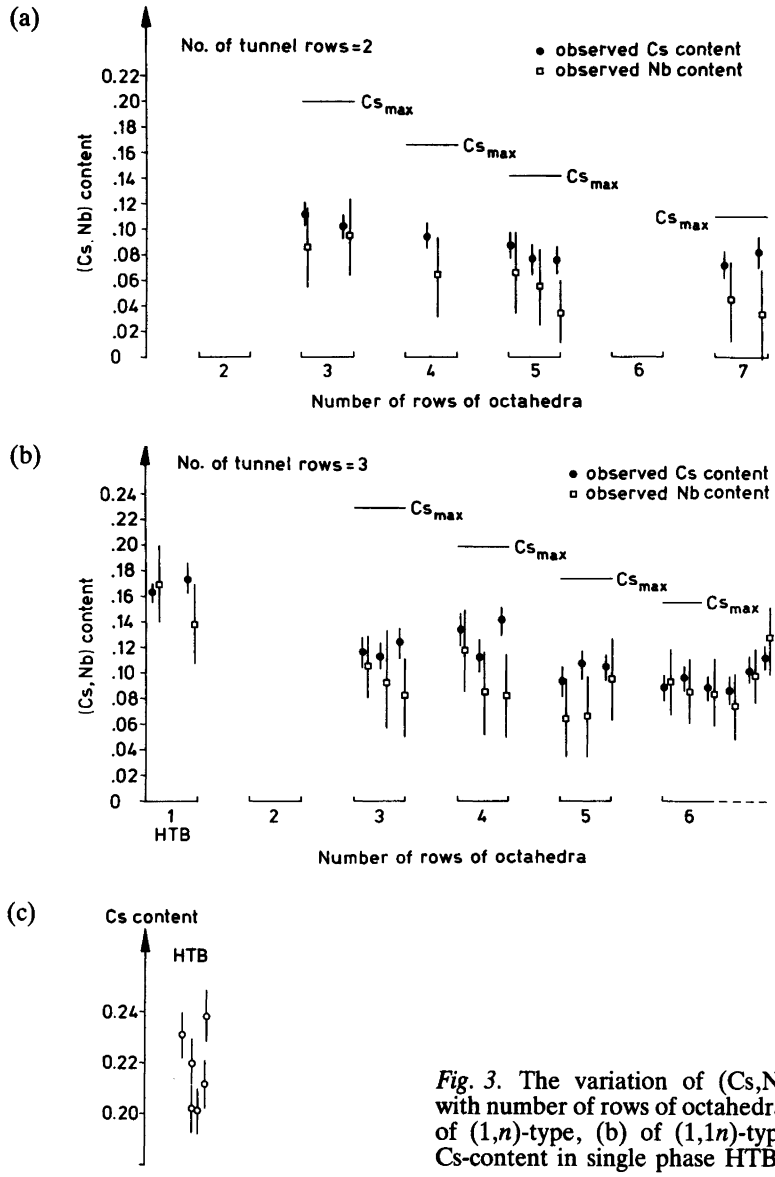

Fig. 3. The variation of (Cs,Nb) content with number of rows of octahedra in ITB (a) of (1,*n*)-type, (b) of (1,1*n*)-type. (c) The Cs-content in single phase HTB.

RESULTS AND DISCUSSION

The results of the quantitative analysis are summarized in Table 1 and Fig. 3. The HTB type crystal fragments were used to check the method. In this case, single-phase samples could be prepared, and the composition was therefore obtained from the weights of the starting materials. X-values ranging from 0.20 to 0.24 were observed (Fig. 2a). The length of the c axis is rather sensitive to x, and a variation of 0.8 % could be expected over this range.[13] This should give rise to a slight broadening of the 004 powder diffraction line. Such a broadening was not observed, however. It is therefore probable that the majority of the

crystals in the sample have a Cs-content falling in a much narrower range that indicated by the few crystals analysed. The average value of the observed Cs-content is 0.218, rather close to $x=0.20$, the expected value from the preparation.

Ordered ITB crystals with double, triple and quadruple tunnel rows were found in the samples examined, and the width of the WO_3 slabs range from 3–7 octahedra, as seen in Table 1. The theoretical limit for the Cs content (all tunnels completely filled) in these structures range from $x=0.111$ to $x=0.230$. It is seen that all observations are well below the maximum composition and rather close to the values corresponding to ~60 % occupancy, as observed for HTB. The results can be compared in two ways.

(i) Fixed width of HTB slabs and variation in the number of octahedra between them (width of WO_3-type lattice). In this case, it is seen that both for the double tunnel phases, (1,*n*) and the triple tunnel phases, (1,1,*n*), the CS content decreases with increasing number of octahedra, *n*, as seen in Fig. 2b and c. One exception, however, is observed: the average value for the (1,1,3) type is slightly lower than for (1,1,4), but the difference is hardly significant, since the standard deviation for the latter is large (Table 1).

(ii) Fixed width of the WO_3-type slabs and different numbers of tunnel rows separating them (width of HTB-type structure). Here it is observed that the Cs-content decreases with decreasing number of tunnels in the structure. Almost all (1,1,6) and (1,1,1,6) crystals analysed came from the same sample, the one that had been remixed and reheated for a longer period. This sample was more homogeneous than those heated for shorter peroids of time.

A few HTB-type crystals were found together with ITB in the low-x samples. The Cs-content of these crystals was slightly lower than that of the single-phase sample (Tab. 1). This indicates that the composition range for HTB extends somewhat below $x=0.20$.

The Nb content determined is, with a few exceptions lower than the corresponding Cs value. As mentioned above, the analysis is rather uncertain, due to partial overlap between the Nb*L* and W*M* peaks, and is quite possible that the error is systematic. Equal amounts of Cs and Nb corresponds to fully oxidised species; with lower Nb content the crystals are necessarily reduced. A slight degree of reduction cannot be excluded, but the crystals are light green and translucent, and this is not usually the case for reduced phases. It is interesting to note that for the samples that were remixed and reheated several times, the Nb- and Cs-content are rather similar.

CONCLUSION

The results obtained in this investigation indicate that tunnels are filled to about 60 % occupancy both in HTB-bronzoids and in the corresponding ITB phases. This degree of filling thus appears to be a preferred value. The system seems to adapt to varying alkali-content by forming different structures, with appropriate relative numbers of tunnels, and not by varying the degree of filling in the tunnels. The narrow compositional range and low occupancy of the tunnels in these phases, compared to earlier results,[5,6] is probably associated with the high temperature of preparation (1200 °C).

Energy dispersive X-ray analysis can aid in finding the composition of the microcrystals of different phases present in the same batch. From the above results we can conclude that the composition, especially the amount of alkali present, has a direct relation to the structure, in this case to the width of the HTB-type slabs. Unfortunately, micro-analysis results have not been reported for the true ITB phases. That type of study of the ITB phases may therefore contribute to a better understanding of the system.

Acknowledgements. I am grateful to professor Lars Kihlborg for his continuous interest and valuable discussions throughout the work. I am also thankful to Mr. Tomasz Nikleweski for his technical assistance with the analyses. This investigation forms a part of a research project financially supported by the Swedish National Science Research Council.

REFERENCES

1. Magnéli, A. *Acta Chem. Scand. 7* (1953) 315.
2. Hussain, A. and Kihlborg, L. *Acta Crystallogr. A 32* (1976) 551.
3. Kihlborg, L. In Metselaar, R., Heijiligers, H.J.M. and Schoonman, J., Eds., *Solid State Chem. 1982, Proc. 2nd Europ., Veldhoven, 7–9th June 1982,* Elsevier, Amsterdam 1983, p. 143.
4. Kihlborg, L. and Sharma, R. *J. Microsc. Spectrosc. Electron. 7* (1982) 387.
5. Deschanvres, A., Frey, M., Raveau, B. and Thomazeau, *J. Bull. Soc. Chim. Fr. 9* (1968) 3519.
6. Darriet, B. and Galy, J. *C.R. Acad. Sci. (Paris) Ser. C 273* (1971) 1173.
7. Sharma, R. and Kihlborg, L. *Mat. Res. Bull. 16* (1981) 377.
8. Hussain, A. *Acta Chem. Scand. A 32* (1978) 479.
9. Iijima, S. *Acta Cryst. A 29* (1973) 165.
10. Statham, P.J. *J. Microsc. 123* (1981) 1.
11. Cheetham, A.K. and Skarnulis, A.J. *Anal. Chem. 53* (1981) 1060.
12. Morris, P.L. *Programme Manual of RTS 2/FLS,* The LINk Systems Ltd., 1979. Appendix 3.
13. Sharma, R. *To be published.*

Received December 19, 1984.